

General-Purpose Parallel Simulator for Quantum Computing

Jumpei Niwa*
niwa@is.s.u-tokyo.ac.jp

Keiji Matsumoto†
keiji@qci.jst.go.jp

Hiroshi Imai*†
imai@is.s.u-tokyo.ac.jp

November 9, 2018

Abstract

With current technologies, it seems to be very difficult to implement quantum computers with many qubits. It is therefore of importance to simulate quantum algorithms and circuits on the existing computers. However, for a large-size problem, the simulation often requires more computational power than is available from sequential processing. Therefore, the simulation methods using parallel processing are required.

We have developed a general-purpose simulator for quantum computing on the parallel computer (Sun, Enterprise4500). It can deal with up-to *30 qubits*. We have performed Shor's factorization and Grover's database search by using the simulator, and we analyzed robustness of the corresponding quantum circuits in the presence of decoherence and operational errors. The corresponding results, statistics and analyses are presented.

key words : quantum computer simulator, Shor's factorization, Grover's database search, parallel processing, decoherence and operational errors

1 Introduction

With the current technologies, it seems to be very difficult to implement quantum computers with many qubits. It is therefore of importance to simulate quantum algorithms and circuits on the existing computers. The purpose of the simulation is

- to investigate quantum algorithms behavior.
- to analyze performance and robustness of quantum circuits in the presence of decoherence and operational errors.

However, simulations often require more computational power than is usually available on sequential computers. Therefore, we have developed the simulation method for parallel computers. That is, we have developed a general-purpose simulator for quantum algorithms and circuits on the parallel computer, Symmetric Multi-Processor.

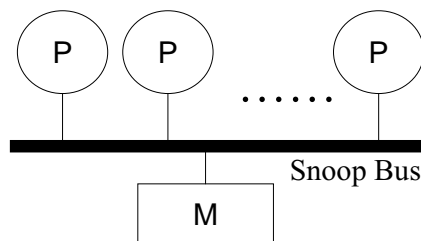


Figure 1: SMP (Symmetric Multi-Processors).

* Department of Computer Science, Graduate School of Information Science and Technology, The University of Tokyo, 7-3-1 Hongo, Bunkyo-ku, Tokyo 113-0033, Japan.

† Quantum Computation and Information Project, ERATO, Japan Science and Technology Corporation, 5-28-3 Hongo, Bunkyo-ku, Tokyo 113-0033, Japan.

to a processor p ($0 \leq p < 2^P$). That is, the processor p computes 2^{i-P} submatrix-subvector multiplications, and the rests of multiplications are performed in other processors in parallel. After each processor has finished its assigned computations, it executes a synchronization primitive, such as the barrier, to make its modifications to the vector (ϕ) , that is, the state of the register visible to other processors.

$$X|\phi\rangle = \left(\begin{array}{cccc} S_0 & & & \mathbf{0} \\ & S_1 & & \\ & & \dots & \\ \hline & & & \dots \\ & & & \dots \\ \hline \mathbf{0} & & & S_{2^i-2} \\ & & & S_{2^i-1} \end{array} \right) \left\{ \begin{array}{l} \left(\begin{array}{c} \phi_0 \\ \phi_1 \\ \dots \\ \dots \\ \dots \\ \phi_{2^i-2} \\ \phi_{2^i-1} \end{array} \right) \end{array} \right\} \left. \begin{array}{l} (processor\ 0) \\ \dots \\ \dots \\ \dots \\ (processor\ 2^P) \end{array} \right\} \quad \text{where } \phi_k = \left(\begin{array}{c} \alpha_{k2^{n-i}} \\ \alpha_{k2^{n-i}+1} \\ \dots \\ \alpha_{(k+1)2^{n-i}-2} \\ \alpha_{(k+1)2^{n-i}-1} \end{array} \right) \quad (0 \leq k < 2^i)$$

Figure 4: Computation decomposition in the general case.

When the number of submatrices is smaller than the number of processors (i.e., $2^i < 2^P$), it is inefficient to assign the computation $M_k (= S_k \phi_k, 0 \leq k < 2^i)$ to one processor as described above. It can cause a load imbalance in the simulation system. In this case, we should decompose the computation M_k itself to improve parallel efficiency. Each submatrix S_k is divided into 2^{P+1} chunks of rows. Each chunk of rows R_j ($0 \leq j < 2^{P+1}$) contains the contiguous $2^{n-i-(P+1)}$ rows of S_k . The multiplications using the chunk of rows R_j and R_{2^P+j} are assigned to a processor j as described in the Figure 5. This decomposition is applied to all the M_k computations ($0 \leq k < 2^i$).

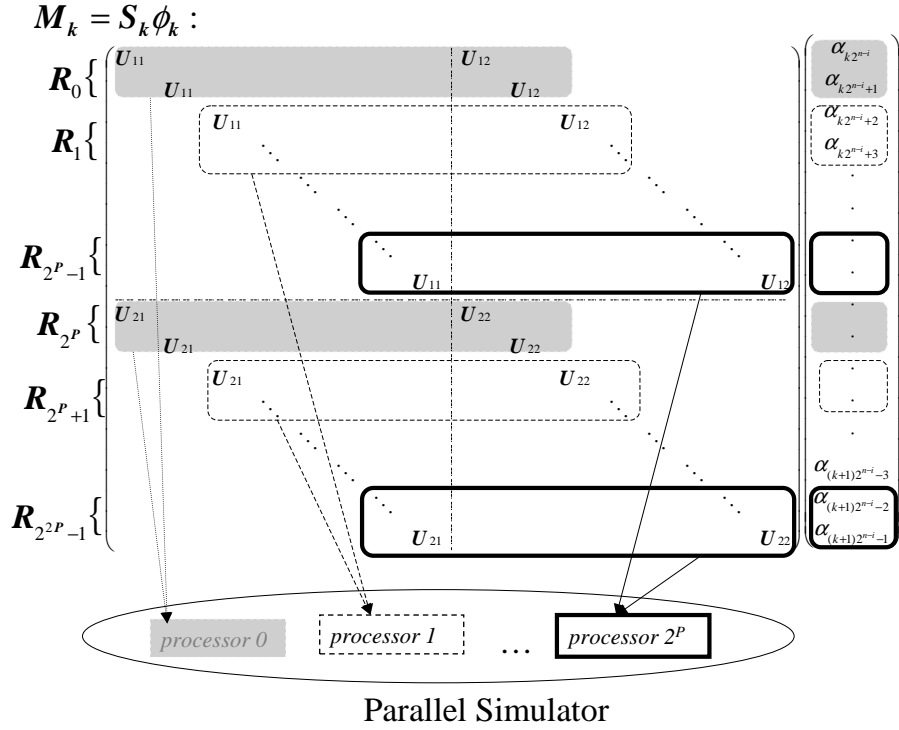


Figure 5: Computation decomposition in the large subblock case.

Note that the computation using j -th row of the submatrix must be always paired with that using $(j + 2^{n-i-1})$ -th row when we use an “in-place” algorithm (i.e., The results of $X|\phi\rangle$ are stored in $|\phi\rangle$). That is, multiplications using the chunk of rows R_j and R_{2^P+j} are assigned to the same processor j . This is because there are dependencies across processors. Consider the following example.

$$\begin{bmatrix} xu_{11} + yu_{12} \\ \dots \\ \dots \\ xu_{21} + yu_{22} \\ \dots \\ \dots \end{bmatrix} = \begin{bmatrix} u_{11} & \dots & \mathbf{0} & u_{12} & \dots & \mathbf{0} \\ \mathbf{0} & \dots & u_{11} & \mathbf{0} & \dots & u_{12} \\ u_{21} & \dots & \mathbf{0} & u_{22} & \dots & \mathbf{0} \\ \mathbf{0} & \dots & u_{21} & \mathbf{0} & \dots & u_{12} \end{bmatrix} \begin{bmatrix} x \\ \dots \\ \dots \\ y \\ \dots \\ \dots \end{bmatrix}$$

If the 1-st element is computed and the result $(xu_{11} + yu_{12})$ is stored before the 4-th element is computed, the result of 4-th element computation becomes not $xu_{21} + yu_{22}$ but $(xu_{11} + yu_{12})u_{21} + yu_{22}$. This is wrong. To avoid this situation, all the processors have only to execute barrier operations before storing the computed results. However, a barrier operation per store operation can cause heavy overheads.

Therefore, the 1-st element computation and 4-th element computation should be assigned to the same processor. Then, the data-dependencies are not cross-processor but in-processor. First, the processor computes $xu_{11} + yu_{12}$ and stores the result in a temporary variable t_1 on the local storage-area (i.e., stack). Second, the processor itself computes the result $xu_{21} + yu_{22}$ and stores it in the 4-th element. Third, the processor stores the contents of the temporary variable t_1 in the 1-st element. In this way, we can avoid the above wrong situation without performing synchronization primitives. If there are no overheads for parallel execution, the time complexity is thus reduced to $O(2^{n-P})$ where 2^P is the number of processors available in the system.

2.2.2 A Controlled Qubit Gate

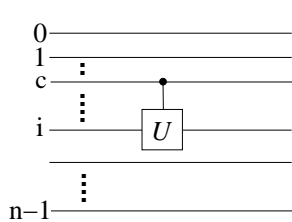


Figure 6: Controlled qubit gate.

Suppose that a unitary matrix $U = \begin{pmatrix} u_{11} & u_{12} \\ u_{21} & u_{22} \end{pmatrix}$ is applied to the i -th qubit if and only if the c -th bit (controlled bit) is 1. Let CTX be the overall unitary matrix ($2^n \times 2^n$). First, we consider the matrix X mentioned in Sec.2.2.1 as if there were no controlled bits. Then, for each j ($0 \leq j < 2^n - 1$), the j -th row of CTX ($CTX[j]$) is defined as follows.

$$CTX[j] = \begin{cases} X[j] & \text{the } c\text{-th bit in } j \text{ is } 1 \\ I[j] & \text{the } c\text{-th bit in } j \text{ is } 0 \end{cases}$$

where I is the unit matrix. In this case, we also do not have to generate CTX or X explicitly. We have only to store the 2×2 matrix U . In many controlled bit cases, it is easy to extend this method. The evolution step is executed in parallel as described in Sec 2.2.1. Therefore, the simulation time is $O(2^{n-P})$ when there are no overheads for parallel execution (2^P is the number of processors available in the simulation system.)

The simulator provides a f -controlled U gate. It is similar to the controlled U gate. The U gate is applied to the target bit iff $f(c) = 1$ (the c -th bit is the controlled bit). It is used in the Grover's Search Algorithm [3].

2.2.3 Measurement Gates

The measurement step for an n -qubit register state is simulated in $O(2^n)$ time as follows. Let $|\phi\rangle = \sum_{j=0}^{2^n-1} \alpha_j |j\rangle$ be an n -qubit register state.

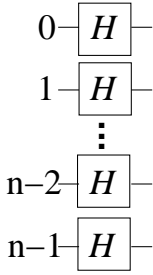
1. Generate a random number r ($0 \leq r < 1$)
2. Determine an integer i ($0 \leq i \leq 2^n - 1$), s.t.

$$\sum_{j=0}^{i-1} |\alpha_j|^2 \leq r < \sum_{j=0}^i |\alpha_j|^2$$

We consider that the measurement is done with respect to the standard basis $|i\rangle$.

2.3 Basic Circuits

2.3.1 Hadamard Transform



The Hadamard transform H_n is defined as follows,

$$H_n|x\rangle = \frac{1}{\sqrt{2^n}} \sum_{y \in \{0,1\}^n} (-1)^{x \cdot y} |y\rangle,$$

for $x \in \{0,1\}^n$. H_n is implemented by the circuit in Figure 7, where \mathbf{H} denotes $\frac{1}{\sqrt{2}} \begin{pmatrix} 1 & 1 \\ 1 & -1 \end{pmatrix}$. Note that it requires $O(n2^{n-P})$ time when there are no overheads for parallel execution (2^P is the number of processors available in the simulation system.).

Figure 7: Hadamard circuit.

2.3.2 Quantum Fourier Transform

The quantum Fourier transform (QFT) is a unitary operation that essentially performs the DFT on quantum register states. The QFT maps a quantum state $|\phi\rangle = \sum_{x=0}^{2^n-1} \alpha_x |x\rangle$ to the state $\sum_{x=0}^{2^n-1} \beta_x |x\rangle$, where

$$\beta_x = \frac{1}{\sqrt{2^n}} \sum_{y=0}^{2^n-1} \omega^{xy} \alpha_y, \quad \omega = e^{2\pi i/2^n}$$

The circuit implementing the QFT is described in the Figure 8. \mathbf{H} is the Hadamard gate, and \mathbf{R}_d is the phase shift gate denoted as $\begin{pmatrix} 1 & 0 \\ 0 & e^{i\pi/2^d} \end{pmatrix}$.

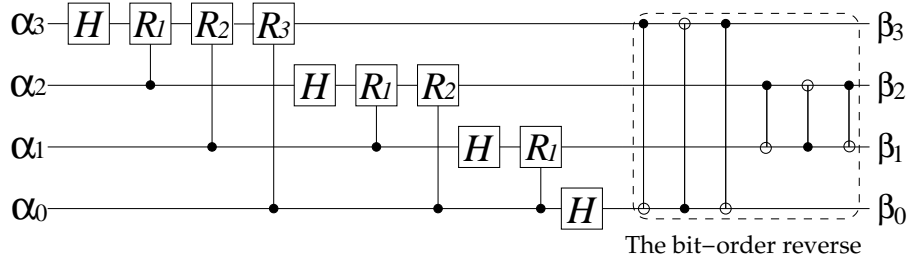


Figure 8: The QFT_{2^n} circuit ($n = 4$).

For general n , this circuit has $O(n^2)$ size*. Therefore, the evolution step is simulated in $O(n^2 2^{n-P})$ time when there are no overheads for parallel execution (There are 2^P processors available in the system). Of course, we can reduce the circuit size to $O(n \log(n/\epsilon))$ [1, 2] if we settle the implementation of fixed accuracy (ϵ), because the controlled phase shift gates acting on distantly separated qubits contribute only exponentially small phases. In this case, the evolution step is simulated in $O(n \log(n/\epsilon) 2^{n-P})$ when there are no overheads for parallel execution.

If we regard the QFT transform as a *black box operator* (that is, if we suppose that this QFT circuit has no error), we do not have to use this quantum circuit in the simulator to perform QFT transformation. We can use fast Fourier transform (FFT) in the simulator instead of the QFT circuit. The FFT algorithm requires only $O(n 2^{n-P})$ steps when there are no overheads for parallel execution. Of course, the FFT gives the exact solution. We use the 8-radix in-place FFT algorithm.

2.3.3 Arithmetical circuits

The arithmetical circuits are important for quantum computing [10]. In the Shor's factoring algorithm[8], the arithmetical circuits to compute modular exponentiation are used. Therefore, according to Ref [4], we

*There is a quantum circuit that computes QFT (modulo 2^n) that has the size $O(n(\log n)^2 \log \log n)$ [2]

have implemented the modular exponentiation circuit by using constant adders, constant modular adders and constant multipliers. $x^a \pmod N$ can be computed using the decomposition,

$$x^a \pmod N = \prod_{i=0}^{l-1} \left((x^{2^i})^{a_i} \pmod N \right), \quad a = \sum_{i=0}^{l-1} a_i 2^i (= a_{l-1} a_{l-2} \dots a_0 \text{ (binary representation)})$$

Thus, modular exponentiation is just a chain of products where each factor is either 1 ($a_i = 0$) or x^{2^i} ($a_i = 1$). Therefore, the circuit is constructed by the pairwise controlled constant multipliers[†].

Let N be an n bit number, and a a $2n$ bit number (that is, l is equal to $2n$ in the above equation.) in the Shor's factoring algorithm because a is as large as N^2 . $n + 1$ qubits are required as the work-space for the controlled multiplier and $n + 4$ for the controlled adders. The total number of required qubits becomes $5n + 6$.

The circuit is constructed with the $O(l)$ (that is, $O(n)$) pairwise controlled constant multipliers. The controlled constant multiplier consists of $O(n)$ controlled constant modular adders. The controlled constant modular adder consists of 5 controlled constant adders. The controlled constant adder consists of $O(n)$ XOR (C-NOT) gates. Thus, the modular exponentiation circuit requires $O(n^3)$ gate. Detailed are described in Ref [4]. It is simulated in $O(n^3 2^{n-P})$ when there are no overheads for parallel execution (2^P is the number of processors available in the simulation system).

3 Error Model

3.1 Decoherence

We consider the quantum depolarizing channel as the decoherence error model. In this channel, with probability $1 - p$, each qubit is left alone. In addition, there are equal probabilities $p/3$ that σ_x , σ_y , or σ_z affects the qubit.

3.2 Operational Error

In general, all of single qubit gates are generated from *rotations*

$$U_R(\theta) = \begin{pmatrix} \cos \theta & -\sin \theta \\ \sin \theta & \cos \theta \end{pmatrix},$$

and *phase shifts*,

$$U_{P1}(\phi) = \begin{pmatrix} 1 & 0 \\ 0 & e^{i\phi} \end{pmatrix} \text{ and } U_{P2}(\phi) = \begin{pmatrix} e^{i\phi} & 0 \\ 0 & 1 \end{pmatrix}.$$

For example, we consider H_n as $U_R(\frac{\pi}{4})U_{P1}(\pi)$, and NOT gate as $U_R(\frac{\pi}{2})U_{P1}(\pi)$. The simulator represents inaccuracies by adding small deviations to the angles of rotation θ and ϕ . Each error angle is drawn from Gaussian distribution with the standard deviation (σ).

4 Preliminary Experiment

We describe the simulation environment and some experiments about basic quantum circuits.

4.1 Simulation Environment

We have developed the simulator on the parallel computer, Sun Enterprise 4500 (E4500). The E4500 has 8 UltraSPARC-II processors (400MHz) with 1MB E-cache and 10GB memory. The system clock is 100MHz. The OS is Solaris 2.8 (64bit OS). The simulator is written in a C language and the compiler that we use is Forte Compiler 6.0. The compiler option “-x05 -fast -xtarget=ultra2 -xarch=v9”. We use the solaris thread library for multi-processor execution. Under this environment, if we use an in-place algorithm, *30-qubit quantum register states can be simulated.*

4.2 Quantum Fourier Transform

Table 1 shows the QFT execution time by the simulator using the QFT-circuit and (classical) FFT algorithm. The numerical error value is ranged from 10^{-15} to 10^{-14} . Recall that 2^P be the number of processors available

[†]Of course, we must classically compute the numbers $x^{2^i} \pmod N$

Table 1: QFT execution time (sec).

| Qubits | Algorithm | Num. of Procs | | | |
|--------|-----------|---------------|---------|---------|---------|
| | | 1 | 2 | 4 | 8 |
| 20 | Circuit | 26.08 | 7.25 | 5.01 | 5.33 |
| | FFT | 1.21 | 0.92 | 0.72 | 0.53 |
| 22 | Circuit | 124.78 | 66.96 | 38.03 | 23.40 |
| | FFT | 5.01 | 3.71 | 2.79 | 1.83 |
| 24 | Circuit | 643.02 | 331.98 | 183.01 | 137.7 |
| | FFT | 20.00 | 12.61 | 8.40 | 5.84 |
| 26 | Circuit | 2745.56 | 1469.73 | 799.57 | 526.82 |
| | FFT | 113.29 | 73.08 | 48.39 | 32.84 |
| 28 | Circuit | 12597.8 | 6738.13 | 3661.51 | 2338.19 |
| | FFT | 567.19 | 319.16 | 205.98 | 142.01 |
| 29 | Circuit | 31089.6 | 16790.6 | 9189.68 | 5811.49 |
| | FFT | 1232.16 | 697.68 | 423.00 | 286.29 |

in the simulation system. The FFT algorithm requires $O(n2^{n-P})$ steps and the QFT circuit requires $O(n^22^{n-P})$ steps for the n -qubit quantum register, if there are no overheads for parallel execution. The execution time is increased in exponential order in proportional to n . The execution time of the FFT is about 20 ~ 30 times as fast as that of the circuit. Both the execution time are decreased when the number of processors are increased. The speedup-ratios on 8-processor execution are about 4 ~ 5. The reason why the speedup-ratios on 8-processor execution are not 8 is that the parallel execution has some overheads that single processor execution does not have. The parallel execution overheads are operating system overheads (multi-threads creation, synchronization, and so on), load imbalance, memory-bus saturation, memory-bank conflict, false sharing and so on. For small-size problems, the ratio of overheads to the computation for parallel execution is relatively large and speedup-ratios on multi-processor execution may be less than 4. The decoherence and operational errors experiment for the QFT is described in Section 5.

4.3 Hadamard Transform

Table 2: HT execution time (sec).

| Qubits | Num. of Procs | | | |
|--------|---------------|--------|--------|--------|
| | 1 | 2 | 4 | 8 |
| 20 | 2.38 | 1.18 | 0.76 | 0.40 |
| 22 | 10.85 | 5.73 | 3.20 | 1.35 |
| 24 | 46.94 | 24.96 | 13.40 | 9.58 |
| 26 | 205.81 | 109.97 | 58.83 | 38.71 |
| 28 | 887.40 | 467.71 | 253.82 | 167.31 |
| 29 | 2027.9 | 1081.1 | 592.08 | 395.81 |

Table 2 shows the Hadamard Transform (HT) execution time by using the circuit. The HT circuit requires $O(n2^{n-P})$ steps for the n -qubit quantum register. The speedup-ratio on 8-processor execution becomes about 5.

4.3.1 Effect of Errors

We have investigated the decrease of the $|0\rangle\langle 0|$ term in the density matrix for the 20-qubit register.

Decoherence Errors

We have analyzed decoherence in the HT circuit on the depolarizing channel. Of course, the simulation deals with pure states. Therefore, the experiments were repeated 10000 times and we use the average values. Each experiment uses different initial random seed. The start state of the quantum register is $|00\dots 0\rangle = |0\rangle$. The HT circuit is applied to the quantum register over and over. The x-axis in the Figure 9 shows the even iteration number. If there are no errors (i.e., the error probability is 0) and the number of iteration is even, the state

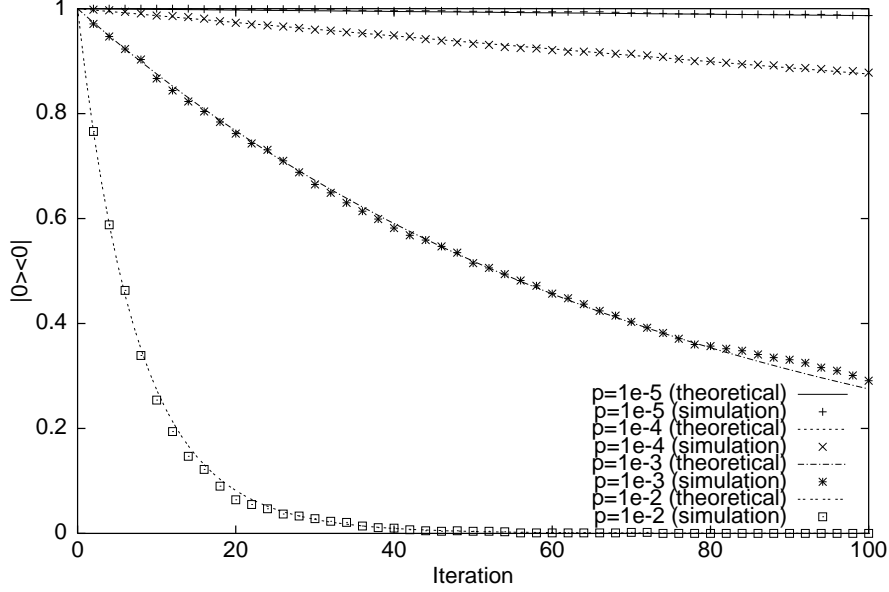


Figure 9: Decrease of the $|0\rangle\langle 0|$ term in the density matrix (20 qubits).

remains $|0\rangle$ and $|0\rangle\langle 0|$ term in the density matrix remains 1. Figure 9 shows how decoherence errors degrade the $|0\rangle\langle 0|$ term. The noise degrades the $|0\rangle\langle 0|$ term significantly if the error probability is greater than 10^{-3} . When the error probability is 10^{-2} , the $|0\rangle\langle 0|$ term is decreased in exponential order in proportional to the number of iterations.

In this easy case, we can compute $|0\rangle\langle 0|$ term in the density matrix theoretically. First, consider the 1 qubit case. Let p be the error probability and ρ_k be the density matrix after the HT circuit is applied to the quantum register k times. The density matrix ρ_{k+1} is calculated as follows.

$$\rho_{k+1} = (1-p)H\rho_k H^* + \frac{p}{3}\sigma_x H\rho_k H^* \sigma_x^* + \frac{p}{3}\sigma_y H\rho_k H^* \sigma_y^* + \frac{p}{3}\sigma_z H\rho_k H^* \sigma_z^*.$$

When the start state of the quantum register is $|0\rangle$ and k is even. ρ_k is calculated as follows,

$$\rho_k = \frac{1}{2} \begin{pmatrix} 1 + (1 - \frac{4}{3}p)^k & 0 \\ 0 & 1 - (1 - \frac{4}{3}p)^k \end{pmatrix}.$$

In the n -qubit case, we can calculate the density matrix similarly when the start state of the quantum register is $|0, \dots, 0\rangle$ and k is even. $|0\rangle\langle 0|$ term of ρ_k is

$$\left(\frac{1 + (1 - \frac{4}{3}p)^k}{2} \right)^n.$$

Figure 9 also shows this theoretical value of $|0\rangle\langle 0|$ term in the density matrix when $p = 10^{-5} \sim 10^{-2}$ and $n = 20$. We can see that the simulations and the theoretical computations yield almost the same result.

Operational Errors

The simulator represents inaccuracies by adding small deviations to the two angles of rotations. Since $H = \mathbf{U}_R(\frac{\pi}{4})\mathbf{U}_{P1}(\pi)$, we add small deviations x and y to $\frac{\pi}{4}$ and π respectively. That is, we use $H(x, y) = \mathbf{U}_R(\frac{\pi}{4} + x)\mathbf{U}_{P1}(\pi + y)$ as the H gate in this experiment. x and y are drawn from Gaussian distribution with the standard deviation (σ). As mentioned above, the experiments are executed 10000 times and we use the average value. Each experiment uses different initial random seed. Figure 10 shows how operational errors degrade the $|0\rangle\langle 0|$ term when $\sigma = 10^{-5} \sim 10^{-2}$ and $n = 20$. The $|0\rangle\langle 0|$ term is not affected by the operational error if σ is less than 10^{-2} .

In this case, we can also compute $|0\rangle\langle 0|$ term in the density matrix theoretically. First, consider the 1 qubit case. Let ρ_k be the density matrix after the HT circuit is applied to the quantum register k times. The density matrix ρ_{k+1} is calculated as follows.

$$\rho_{k+1} = \int_{-\infty}^{\infty} \int_{-\infty}^{\infty} H(x, y)\rho_k H(x, y)^* p(x)p(y) dx dy$$

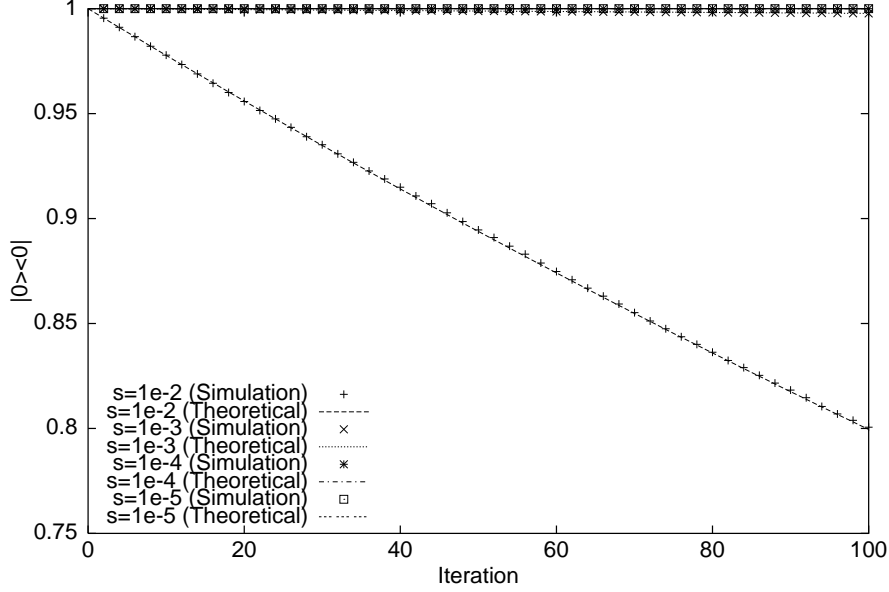


Figure 10: Decrease of the $|0\rangle\langle 0|$ term in the density matrix (20 qubits).

where $p(z) = \frac{1}{\sqrt{2\pi}\sigma} e^{-\frac{z^2}{2\sigma^2}}$. When the start state of the quantum register is $|0\dots 0\rangle = |0\rangle$, ρ_k is calculated as follows,

$$\rho_k = \frac{1}{2} \begin{pmatrix} 1 + e^{-\frac{\sigma^2}{4}9k} & 0 \\ 0 & 1 - e^{-\frac{\sigma^2}{4}9k} \end{pmatrix}.$$

As for the general n -qubit case, we can calculate the density matrix similarly when the start state of the quantum register is $|0\dots, 0\rangle$ and k is even. $|0\rangle\langle 0|$ term of ρ_k is

$$\left(\frac{1 + e^{-\frac{\sigma^2}{4}9k}}{2}\right)^n.$$

Figure 9 also shows this theoretical value of $|0\rangle\langle 0|$ term in the density matrix when the standard deviation $\sigma = 10^{-5} \sim 10^{-2}$ and $n = 20$. It follows from the theoretical computation that $|0\rangle\langle 0|$ term is decreased in exponential order in proportional to the number of iterations k .

Both Operational and Decoherence Errors

Table 3: Combined effects for HT.
Operational(σ)

| | 0 | 10^{-5} | 10^{-4} | 10^{-3} |
|-----------|--------|-----------|-----------|-----------|
| 0 | 1.0000 | 1.0000 | 0.9999 | 0.9977 |
| 10^{-5} | 0.9870 | 0.9870 | 0.9849 | 0.9797 |
| 10^{-4} | 0.9010 | 0.9010 | 0.8909 | 0.8780 |
| 10^{-3} | 0.2910 | 0.2790 | 0.2779 | 0.2664 |

Each element of Table 3 represents the $|0\rangle\langle 0|$ term of the density matrix after the HT is applied to the state $|0\rangle$ of a 20-qubit register 10000 times. The combined effect of two factors may be worse than each factor alone, that is to say, the effect seems to be the product of each factor. Table 3 shows this situation.

5 Experiment

5.1 Shor's Factorization Algorithm [8, 9]

First, we review the algorithm briefly.

Input An l bit odd number n that has at least two distinct prime factors.

Output A nontrivial factor of n

1. Choose an arbitrary $x \in \{1, 2, \dots, n-1\}$
2. (Classical) Compute $d = \gcd(x, n)$ by using Euclid's algorithm. If $d > 1$, output d and stop.
3. (Quantum) Try to find the order of x :
 - (a) Initialize an l -qubit register and a $2l$ -qubit register to state $|0\rangle|0\rangle$.
 - (b) Apply the HT to the second register.
 - (c) Perform the modular exponentiation operator.
That is, $|0\rangle|a\rangle \rightarrow |x^a \pmod n\rangle|a\rangle$
 - (d) Measure the first register and apply the QFT to the second register and measure it. Let y be the result.
4. (Classical) Find relatively prime integers k and r ($0 < k < r < n$), s.t. $|\frac{y}{2^{2l}} - \frac{k}{r}| \leq \frac{1}{2^{(2l+1)}}$ by using the continued fraction algorithm. If $x^r \not\equiv 1 \pmod n$ or r is odd or $x^{r/2} \equiv \pm 1 \pmod n$, output "failure" and stop.
5. (Classical) Compute $d_{\pm} = \gcd(n, x^{\frac{r}{2}} \pm 1)$ by using Euclid's algorithm. Output numbers d_{\pm} and stop.

When the simulator performs all the step-3 operations (not only the QFT but also the modular exponentiation) on the quantum circuit, $5l + 6$ qubits are totally required, as described in the Section 2.3.3. Therefore, the simulator can only deal with 4-bit integer n ($5l + 6 \leq 30 \rightarrow l \leq 4$). The 4-bit integer that satisfies the input property is only 15. We have tried to factor 15 on the simulator. Beyond our expectation, the modular exponentiation is computationally much heavier than the QFT.

Table 4: Execution time in the Shor's factorization algorithm when $n = 15$ and $x = 11$ (All the quantum operations are executed on the circuit).

| Modular exponentiation | QFT |
|------------------------|---------------|
| 18184 (sec) | 0.64270 (sec) |

The modular exponentiation requires $O(l^3 2^{l-P})$ steps and the QFT on the circuit requires $O(l^2 2^{l-P})$ steps when there are 2^P processors available in the simulation system and there are no overheads for parallel execution. Of course, in the classical computer, modular exponentiation consists of basic operations such as addition, multiplication and division. However, these basic operations are not so heavy in the classical computer, because it has the dedicated non-reversible circuit (the so-called ALU :arithmetic logic unit). This situation suggests that a brand-new fast quantum algorithm for arithmetic operations are required. 15 is not enough to investigate the behavior of Shor's factoring algorithm. To factor much larger number in a reasonable time, the simulator performs the step-3(c) and the step-3(d) classically. That is, the modular exponentiation are computed classically and the QFT is computed by the FFT algorithm in the simulator. In this case, the simulator does not need to generate the first register. Therefore, the simulator can factor about $14 \sim 15$ -bit integers (for example, 23089).

The factoring algorithm successes with the probability greater than

$$\begin{aligned} \text{Prob}_{\text{succ}}(n) &= p_{\text{step2}} + (1 - p_{\text{step2}})p_{\text{step3}\sim 4} \\ &= \left(1 - \frac{\phi(n)}{n-1}\right) + \frac{\phi(n)}{n-1} \cdot \left(\frac{1}{2} \cdot \frac{4}{\pi^2} \frac{e^{-\gamma}}{\log \log n}\right) \end{aligned}$$

where p_{step2} means the probability that the step-2 successes and $p_{\text{step3}\sim 4}$ means the probability that step-3 and the step-4 success and γ is the Euler constant $\phi(n)$ is the Euler number of n . If the above algorithm is repeated $O(1/\text{Prob}_{\text{succ}}(n))$ times, the success probability can be as close to 1 as desired.

We choose an $n = pq$ where p and q are prime numbers. This kinds of integers are chosen in an RSA cryptosystem because it is believed that it is hard to factor such integers easily. $\phi(n) = (p-1)(q-1)$ for such integers. We have experimented with several RSA-type $14 \sim 15$ -bit integers.

The simulator repeats the above algorithm until a nontrivial factor of n is found. The simulator records the number of iterations. The experiment is executed 100 times and we use the average of these recorded iterations. We compare the simulation values with the theoretical number of needed iterations (i.e., $1/\text{Prob}_{\text{succ}}(n)$). The results are shown in the Table 5. Theoretical values (**Theoretical**) are about only $2 \sim 4$ times as large as

Table 5: Number of needed iterations of Shor’s factoring algorithm.

| n | Num. of Iterations | | |
|--------------------|--------------------|------------|----------|
| | Theoretical | Simulation | |
| | | Original | Improved |
| 21311(= 211 · 101) | 15.79 | 6.690 | 1.760 |
| 21733(= 211 · 103) | 15.85 | 8.990 | 2.356 |
| 22999(= 211 · 109) | 16.00 | 6.360 | 1.730 |
| 22523(= 223 · 101) | 15.88 | 5.480 | 1.770 |
| 22927(= 227 · 101) | 15.91 | 3.790 | 1.470 |
| 22969(= 223 · 103) | 15.94 | 8.050 | 2.070 |
| 23129(= 229 · 101) | 15.92 | 7.133 | 1.636 |

simulation values (**Original**). Although much more simulations are required, the theoretical values seem to be fairly good.

As suggested in Ref [9], the algorithm is optimized so as to perform less quantum computation and more (classical) post-processing.

1. *Neighbor y Check*

If we do not find the relatively prime integers k and r by using the continued fraction algorithm, it is wise to try $y \pm 1$, $y \pm 2$.

2. *GCD Check*

Even if $x^r \not\equiv 1 \pmod{n}$, try to compute $d_{\pm} = \gcd(n, x^{\frac{r}{2}} \pm 1)$.

3. *Small Factor Check*

If $x^r \not\equiv 1 \pmod{n}$, it is wise to try $2r, 3r \dots$. This is because if $\frac{y}{2^{2t}} \approx \frac{k}{r}$, where k and r have a common factor, this factor is likely to be small. Therefore, the observed value of $\frac{y}{2^{2t}}$ is rounded off to $\frac{k'}{r'}$ in the lowest terms.

4. *LCM Check*

If two candidates for r , that is r_1 and r_2 , have been found, it is wise to test $\text{lcm}(r_1, r_2)$ as a candidate r .

We have tested how much the algorithm is improved by these modifications. The results are also shown in Table 5 (**Improved**). The number of iterations are reduced to about $1/5 \sim 2/5$. The detailed effect of the improved algorithm is described in Table 6.

Table 6: Detailed effect of improved algorithm

| n | Ratio of Success/Failure | | | |
|-------|--------------------------|--------|-------|--------|
| | 1(Neighbor) | 2(GCD) | 3(SF) | 4(LCM) |
| 21311 | 27/9 | 52/19 | 12/4 | 3/4 |
| 23129 | 27/9 | 52/19 | 12/4 | 3/4 |
| 22999 | 37/6 | 47/79 | 13/8 | 2/58 |
| 22969 | 41/8 | 22/82 | 31/22 | 1/28 |
| 22927 | 25/3 | 35/49 | 18/2 | 1/28 |
| 22523 | 37/6 | 45/76 | 18/22 | 7/54 |

Each element of Table 6 represents s/f where s means the number of success iterations and f means the number of failure iterations. For example, about $n = 23129$, the first optimization, “Neighbor Check” is performed for $27+9 = 36$ iterations and the candidate of the order is found successfully in 27 iterations. It seems that the second optimization “GCD Check” works well for all the n that we have experimented with. From this result, we can see that even if $x^r \not\equiv 1 \pmod{n}$, $d_{\pm} = \gcd(n, x^{\frac{r}{2}} \pm 1)$ often become the factor of n . That is, even

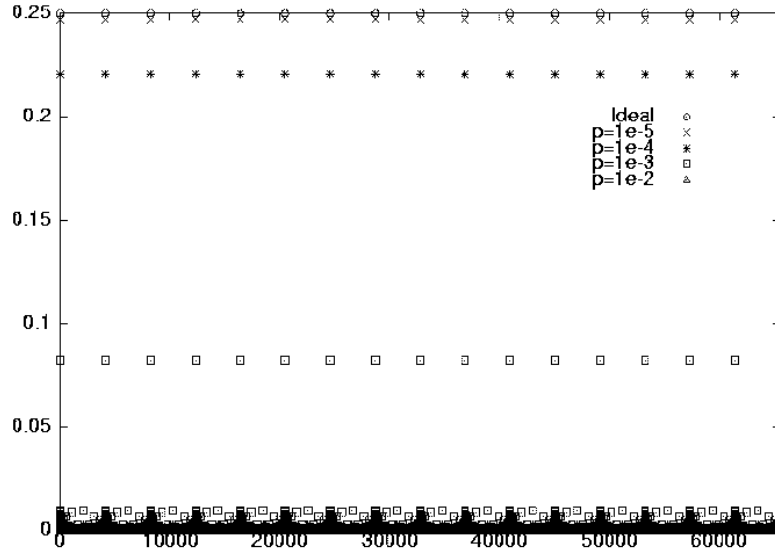
if the candidate r is not equal to $ord(x)$ (an order of x), there is the possibility that $\mathbf{N} \ni \exists a > 1, a \cdot r = ord(x)$. In this case, the following equation holds when r is even.

$$\begin{aligned} 0(\bmod n) &\equiv x^{ord(x)} - 1 \\ &\equiv (x^r - 1)(x^{(a-1)r} + x^{(a-2)r} + \dots + 1) \\ &\equiv (x^{r/2} - 1)(x^{r/2} + 1)(x^{(a-1)r} + x^{(a-2)r} + \dots + 1) \end{aligned}$$

Thus, there is the possibility that n and $x^{\frac{r}{2}} \pm 1$ have a common non-trivial factor.

5.2 Effect of Errors

We have analyzed decoherence and operational errors in the QFT circuit. **Decoherence Errors**



| p | 0 | 10^{-5} | 10^{-4} | 10^{-3} | 10^{-2} |
|------------|--------|-----------|-----------|-----------|-----------|
| Iterations | 1.9569 | 2.1000 | 2.3201 | 6.0606 | 327.00 |

Figure 11: Amplitude amplification by QFT in the presence of decoherence error (top) and the required number of iterations (bottom) (16 qubits).

We assume that each qubit is left intact with probability $1 - p$ and it is affected by each of the error operators $\sigma_x, \sigma_y, \sigma_z$ with the same probability $\frac{p}{3}$ each time the register is applied by the controlled rotation gate \mathbf{R}_d . Figure 11 shows the amplitude amplification phase by the QFT circuit on the depolarizing channel in Shor's factorization algorithm (Step 3 (d)) when $n = 187$ and $x = 23$. The y axis in the Figure 11 shows the amplitude. The experiment is executed 1000 times and we use the average. If the error probability is greater than 10^{-3} , it is hard to use the QFT circuit for the purpose of period estimation.

Operational Errors

The simulator represents inaccuracies by adding small deviations to the angles of rotations of \mathbf{R}_d . We consider $H_n = \mathbf{U}_R(\frac{\pi}{4})\mathbf{U}_{P1}(\pi)$, and NOT gate = $\mathbf{U}_R(\frac{\pi}{2})\mathbf{U}_{P1}(\pi)$. The simulator also represents inaccuracies by adding small deviations to these angles of rotations. The error is drawn from Gaussian distribution with the standard deviation (σ). As mentioned above, the experiment is executed 1000 times and we use the average. Figure 12 shows the amplitude amplification phase by the QFT in the Shor's factorization algorithm (Step 3(d)) when $n = 187$ and $x = 23$. It seems that the period extraction by using the QFT is not affected by the operational error.

Both Operational and Decoherence Errors

We investigate the combined effect of operational and decoherence errors. Table 7 shows the result. Each element of table represents the *fidelity*. The fidelity is defined as the inner product of the correct state and the simulated state with errors.

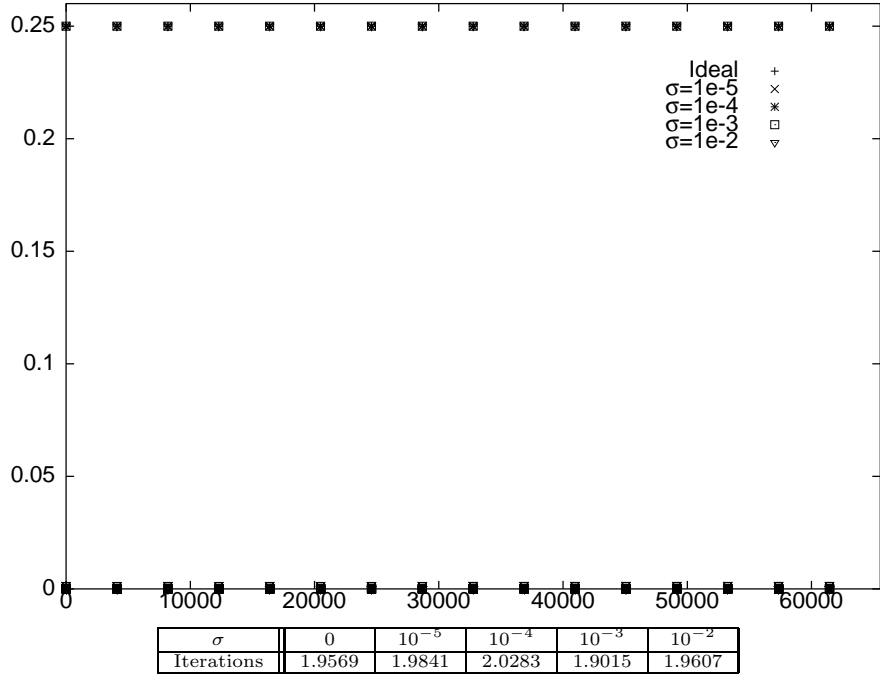


Figure 12: Amplitude amplification by QFT in the presence of operational error (top) and the required number of iterations (bottom) (16 qubits).

The combined effect of two factors may be worse than each factor alone, that is to say, the effect seems to be the product of each factor. However, when the decoherence rate is relatively higher, the small-deviation operational error can improve the results contrary to our expectations. When the size of register is large, the decoherence probability even greater than 10^{-3} drops the fidelity significantly.

Table 7: Combined effects for QFT (16bit)
Operational(σ)

| | 0 | 10^{-5} | 10^{-4} | 10^{-3} | 10^{-2} |
|--------------------|-----------|-----------|-----------|-----------|-----------|
| Decoherence(p) | 0 | 0.9999 | 0.9999 | 0.9999 | 0.9998 |
| | 10^{-5} | 0.9880 | 0.9840 | 0.9860 | 0.9880 |
| | 10^{-4} | 0.8837 | 0.8897 | 0.8827 | 0.8801 |
| | 10^{-3} | 0.3287 | 0.3399 | 0.3332 | 0.3209 |
| | 10^{-2} | 0.0027 | 0.0015 | 0.0019 | 0.0017 |

5.3 Grover's Search Algorithm [3]

Suppose that a function $f_k : \{0, 1\}^n \rightarrow \{0, 1\}$ is an oracle function such that $f_k(x) = \delta_{xk}$. The G-iteration is denoted as $-H_n V_{f_0} H_n V_{f_k}$. The sign-changing operator V_f is implemented by using the f -controlled NOT gate and one ancillary bit. Figure 13 shows the circuit of Grover's algorithm.

5.3.1 Effect of Errors

We have analyzed the impacts of decoherence and operational errors in the circuit of Grover's algorithm. We assume depolarizing channel that each qubit is left intact with probability $1 - p$ and it is affected by each of the error operators $\sigma_x, \sigma_y, \sigma_z$ with the same probability $\frac{p}{3}$ per G-iteration. We consider $H_n = U_R(\frac{\pi}{4})U_{P1}(\pi)$ and NOT-gate = $U_R(\frac{\pi}{2})U_{P1}(\pi)$. The simulator represents inaccuracies by adding small deviations to the angles of these rotations. Each error angle is drawn from Gaussian distribution with the standard deviation (σ).

Figure 14 and 15 show the impacts of errors for a 10-qubit register. The experiments were repeated 1000 times and we use the average values. If there are no errors, plotting the amplitude of the correct element (that is, k) makes a sine curve. However, the amplitudes are decreased as G-iterations are repeated in the presence

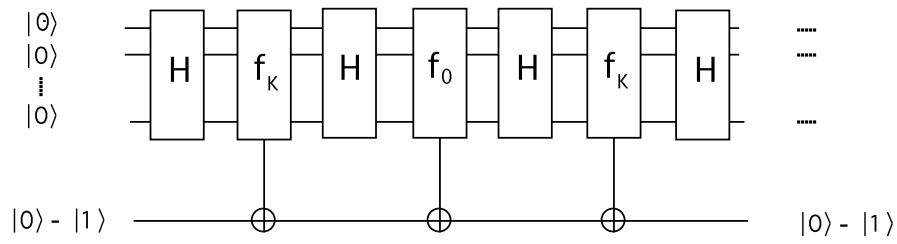


Figure 13: The circuit of Grover's algorithms.

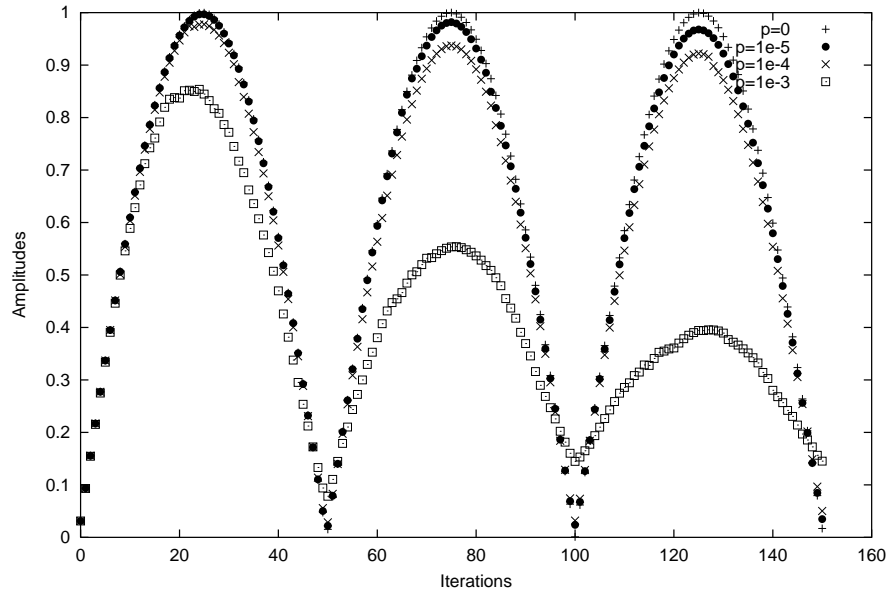


Figure 14: Decrease of the amplitude of the correct element in the presence of decoherence errors (10 qubit).

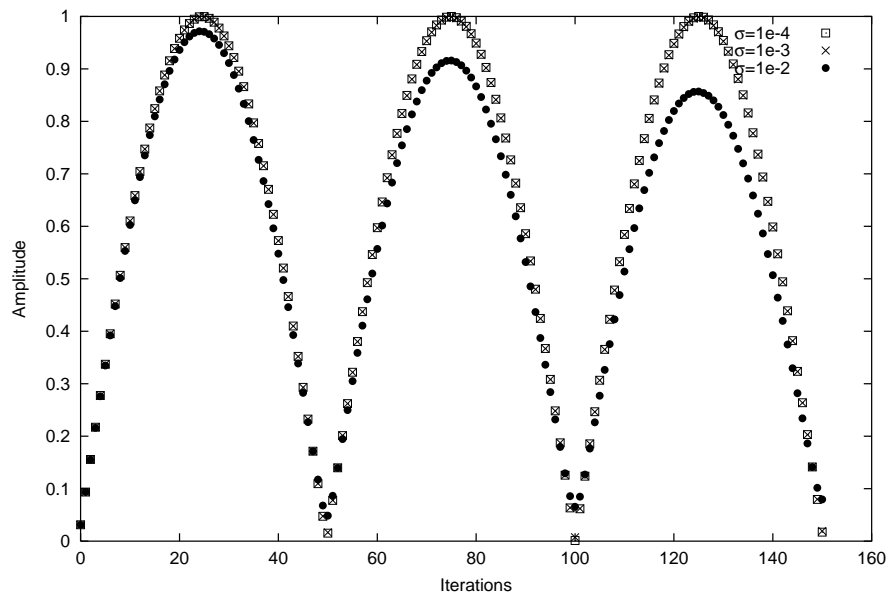


Figure 15: Decrease of the amplitude of the correct element in the presence of operational errors (10 qubit).

of errors. Figure 14 shows the impacts of decoherence error. We can see that the decoherence error affects the period of the sine-curve. Figure 15 shows the impacts of operational errors. It seems that the operational error does not affect the period of the sine-curve.

6 Related Works

There are many quantum simulators for quantum circuit model of computation [5, 7, 6, 11]. QDD[7] aims to use Binary Decision Diagram in order to represent the states of quantum register. QCL[6] and OpenQubit[11] both use complex number representation of the quantum states like our simulator. In addition, QCL tries to establish a high-level, architecture-independent programming language. The Obenland's simulator [5] is based on an actual physical experimental realization and it uses parallel processing like our simulator. Although it runs on the distributed-memory multi-computers, our simulator runs on the shared-memory multi-computers. Therefore, in our simulator, there is no need to distribute and collect the states of the quantum register. In addition, our simulator uses more efficient evolution algorithms and adopts (classical) FFT algorithms for the fast simulation of the large-size problems. Our simulator does not depend on any actual physical experimental realizations because it is not easy to say which realizations are best at this moment. In other words, our simulator is more general-purpose.

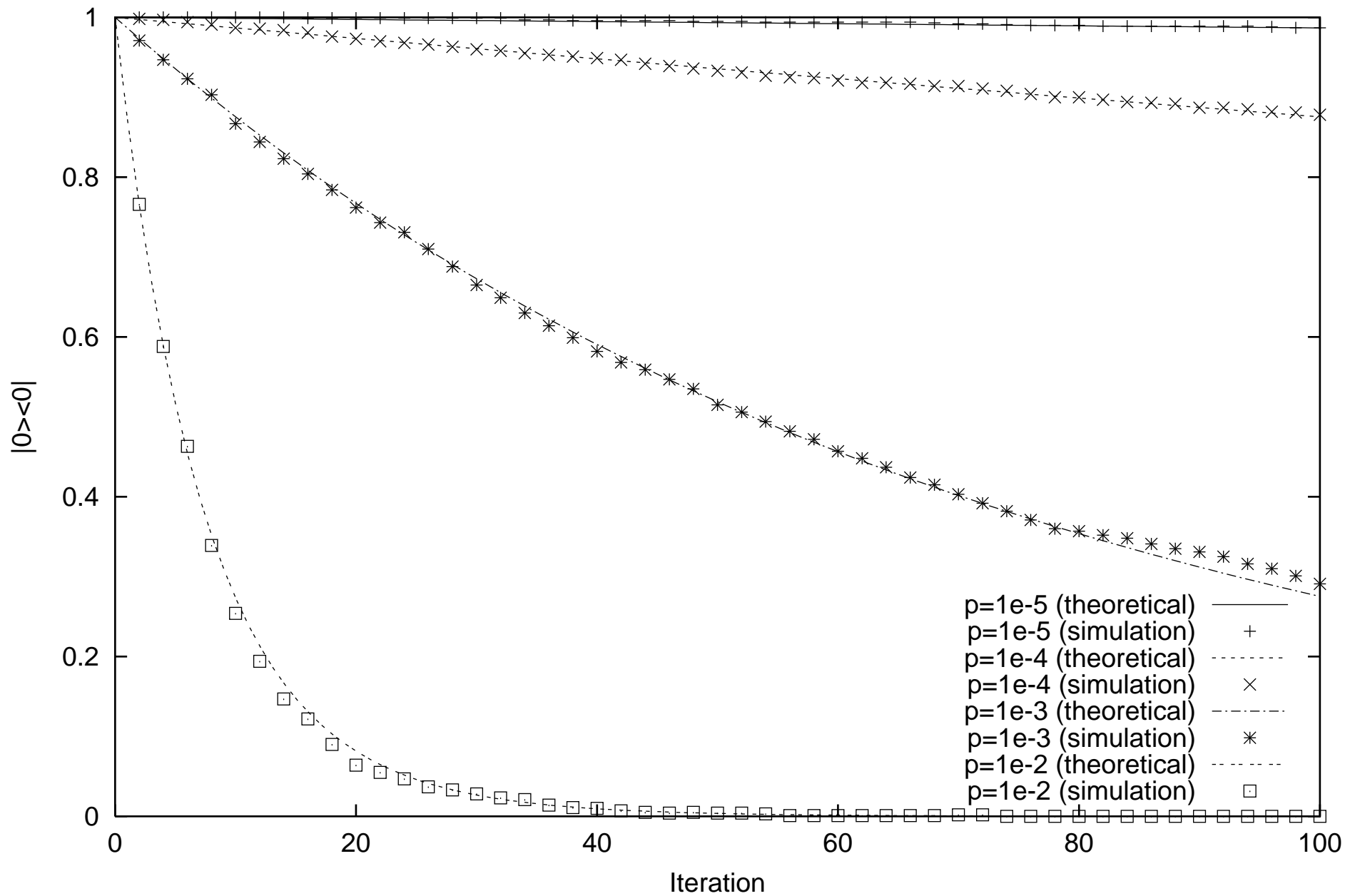
7 Conclusion

We have developed a parallel simulator for quantum computing on the parallel computer (Sun, Enterprise4500). Up-to 30 qubits can it deal with. We have performed Shor's factorization and Grover's database search by using the simulator, and we analyzed robustness of the corresponding quantum circuits in the presence of decoherence and operational errors. If the decoherence rate is greater than 10^{-3} , it seems to be hard to use the both quantum algorithms in practice. For future work, we will investigate the correlation between decoherence and operational errors, that is, why small-deviation operational errors can improve the results when the decoherence rate is relatively higher. Furthermore, we will try quantum error-correcting code to fight decoherence and operational errors.

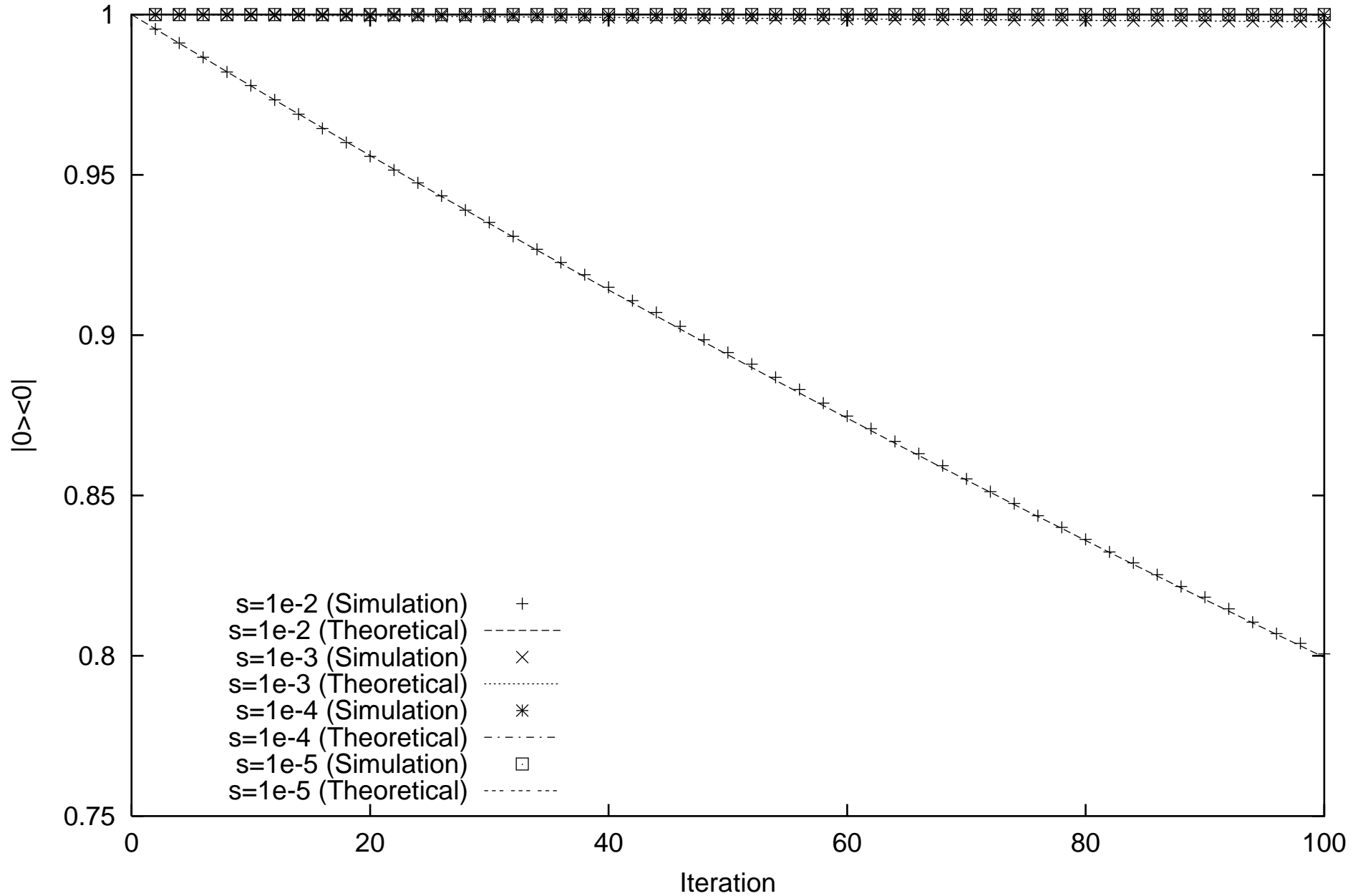
References

- [1] A. Barenco, A. Ekert, K. Suominen, and P. Torma. Approximate quantum fourier transform and decoherence, 1996.
- [2] R. Cleve and J. Watrous. Fast parallel circuits for the quantum fourier transform, 2000.
- [3] Lov K. Grover. A fast quantum mechanical algorithm for database search. In *ACM Symposium on Theory of Computing*, pages 212–219, 1996.
- [4] Cesar Miquel, Juan Pablo Paz, and Roberto Perazzo. Factoring in a dissipative quantum computer. Los Alamos Physics Preprint Archive, <http://xxx.lanl.gov/abs/quant-ph/9601021>, 1996.
- [5] K. Obenland and A. Despain. A parallel quantum computer simulator, 1998.
- [6] Bernhard Ömer. Quantum programming in qcl. Master's thesis, Institute of Information Systems Technical University of Vienna, January 2000.
- [7] QDD ver.0.2, <http://home.plutonium.net/~dagreve/qdd.html>, March 1999.
- [8] Peter W. Shor. Algorithms for quantum computation: Discrete logarithms and factoring. In *IEEE Symposium on Foundations of Computer Science*, pages 124–134, 1994.
- [9] Peter W. Shor. Polynomial-time algorithms for prime factorization and discrete logarithms on a quantum computer. *SIAM Journal on Computing*, 26(5):1484–1509, 1997.
- [10] Vlatko Vedral, Adriano Barenco, and Artur K. Ekert. Quantum networks for elementary arithmetic operations. *Physical Review A*, 54(1):147-153, 1996.
- [11] Jonathan Blow Yan Protzker and Joe Nelson. Openqubit 0.2.0. <http://www.ennui.net/~quantum/>, December 1998.

Decrease of $|0\rangle\langle 0|$ term (20qubits, Hadamard, Decoherence)



Decrease of $|0\rangle\langle 0|$ term (20qubits, Hadamard, Operational (Gauss Dist.))



$S_k |\phi_k\rangle:$

